NASA

Technical Memorandum **86128**

THERMAL BIFURCATION IN THE UPPER SOLAR PHOTOSPHERE INFERRED FROM HETERODYNE SPECTROSCOPY OF OH ROTATIONAL LINES

Drake Deming, John J. Hillman, Theodor Kostiuk, Michael J. Mumma and David M. Zipoy

JUNE 1984

National Aeronautics and
Space Administration

Goddard Space Flight Center
Greenbelt, Maryland 20771

THERMAL BIFURCATION IN THE UPPER SOLAR PHOTOSPHERE

INFERRED FROM HETERODYNE SPECTROSCOPY OF OH ROTATIONAL LINES

Drake Deming[†], John J. Hillman, Theodor Kostiuk[†], and Michael J. Mumma[†]

Infrared and Radio Astronomy Branch
Laboratory for Extraterrestrial Physics
Goddard Space Flight Center

and

David M. Zipoy[†]

Astronomy Program
University of Maryland

To appear in Solar Physics

[†] Visiting Astronomer, Kitt Peak National Observatory, which is operated by the Association of Universities for Research in Astronomy, under contract with the National Science Foundation.

Suggested Running Head: Heterodyne Spectroscopy of OH

ABSTRACT

We have obtained low noise (S/N > 10^3), high spectral resolution ($\nu/\Delta\nu \sim 10^6$) observations of two pure rotation transitions of OH from the solar photosphere. The observations were obtained using the technique of optically null-balanced infrared heterodyne spectroscopy, and consist of center-to-limb line profiles of a v=1 and a v=0 transition near 12μm. These lines should be formed in local thermodynamic equilibrium (LTE), and are diagnostics of the thermal structure of the upper photosphere. We find that the v=0 R22(24.5)e line strengthens at the solar limb, in contradiction to the predictions of current one-dimensional photospheric models. Our data for this line support a two-dimensional model in which horizontal thermal fluctuations of order ± 800K occur in the region $\tau_{5000} \sim 10^{-3} - 10^{-2}$. This thermal bifurcation may be maintained by the presence of magnetic flux tubes, and may be related to the solar limb extensions observed in the 30-200μm region.

Observations of the v=1 R11(29.5)f line, at 885.643 cm^{-1}, show that it is anomalously weak in the photospheric spectrum. We argue that the source function in the core of this line has been substantially increased by interaction with the 9j-7i transition of MgI at 885.524 cm^{-1}, which is itself too weak to appear in the disk center spectrum.

I. INTRODUCTION

Current understanding of the structure of the solar photosphere is based largely upon spectroscopy of its visible region absorption line spectrum. Inferences concerning the upper photosphere are often made from an analysis of the profiles of strong absorption lines, such as the Calcium K-line (Ayres and Linsky 1976). Such lines, however, are normally affected by departures from local thermodynamic equilibrium (LTE). While non-LTE (NLTE) problems are of interest in their own right, a probe of photospheric temperature structure is most useful if the source function can be simply related to the local kinetic temperature through LTE. One way to achieve an LTE diagnostic of the upper photosphere is to observe the solar continuum in the mid-to-far-infared ($10\text{-}500_{\mu}$m). In these regions the H^- free-free opacity increases with wavelength, allowing continuum measurements to probe the upper photosphere (DeJager 1975). Moreover, the infrared continuum from the temperature minimum region is believed to be formed in LTE, unlike the ultraviolet continuum formed in this region (Vernazza et al. 1976). Unfortunately, far infrared measurements of absolute flux are extremely difficult to perform from the ground, due to extensive atmospheric absorption. An attractive alternative is to perform spectroscopy of (mostly molecular) infrared lines, using equivalent width or line profile information to probe a range of height in the upper photosphere. Many of these infrared vibration-rotation, and especially pure rotation, lines are expected to be formed in LTE (e.g. Carbon et al. 1976; Hinkle and Lambert 1975).

Spectroscopy of infrared CO lines, however, has indicated that the upper photosphere ($10^{-4} \leq \tau_{5000} \leq 10^{-2}$) cannot be represented by a one-dimensional model (Ayres and Testerman 1981). Ayres (1981) has proposed that a thermal bifurcation occurs in the outer photosphere, such that cold ($T \lesssim 4000$K) regions are interleaved with regions of much hotter plasma. Ayres identifies the hot regions with magnetic flux tubes (Spruit 1981), and suggests that enhanced transport of acoustic energy heats these regions. Between magnetic flux tubes, Ayres suggests that strong radiative cooling by CO lowers the local kinetic temperature. It has long been known that one-dimensional empirical temperature models are in poor agreement for $\tau_{5000} \lesssim 10^{-2}$; empirical values for the temperature minimum are a strong function of the spectral feature used to derive

the thermal model. This situation strongly hints at the presence of significant thermal inhomogeneities in the region of the temperature minimum.

Recently, Goldman et al. (1981) discovered pure rotation lines of OH from the v=0, 1 and 2 states in the photospheric spectrum near 12μm. The v=0 OH lines were used by Goldman et al. (1983) to derive a new value for the photospheric oxygen abundance, using 0.02 cm^{-1} resolution Fourier Transform Spectrometer (FTS) spectra. Lines from the v=0, 1, 2 and 3 states were observed by Sauval et al. (1984) using 0.005 cm^{-1} resolution spectra taken with the Kitt Peak FTS. Sauval et al. derive an oxygen abundance of 8.91 ± 0.01 from 81 lines. These lines are important indicators of photospheric oxygen abundance for several reasons. First, their f-values can be derived directly from the well-determined dipole moment (Meerts and Dynamus 1969; Mies 1974; Stevens et al. 1974; Werner et al. 1983), and the dissociation energy of OH is precisely known (Carlone and Dalby 1969). Moreover, in the upper photosphere both the rotational and vibrational excitation temperatures of OH should equal the kinetic temperature (see Hinkle and Lambert 1975). These circumstances, which make the OH features useful as abundance indicators, also imply that their line profiles can be used as probes of the upper photospheric thermal structure. Goldman et al. (1983) noted that the principal source of error in their abundance analysis was the uncertainty of the model atmosphere. One way to reduce this uncertainty is to obtain center-to-limb measurements of the line profiles. In this paper we report low noise ($S/N > 10^3$), high spectral resolution ($\nu/\Delta\nu \sim 10^6$) observations of two of these features, and their center-to-limb dependence. We utilize these observations to make inferences concerning the thermal structure and inhomogeneity of the upper photosphere.

II. OBSERVATIONS

a. Heterodyne spectroscopy

The observations were made with the Goddard Infrared Heterodyne Spectrometer interfaced with the McMath main solar telescope at Kitt Peak National Observatory. We used the technique of optically null-balanced infrared heterodyne spectroscopy with a $^{14}C^{16}O_2$ gas laser. This technique has not been previously applied to solar problems. Pioneering efforts in heterodyne

detection of the Sun were made by McElroy (1972), Gay and Journet (1973), and Veth et al. (1973). Tunable diode laser heterodyne spectroscopy of sunspots was recently reported by Glenar et al. (1982). However, heterodyne spectroscopy of solar features, using gas lasers, is new to the literature. We will therefore describe these observations in more detail than is usually appropriate.

Heterodyne spectroscopy of astronomical sources is accomplished by combining source radiation with the output of a laser local oscillator (LO). These coplanar wavefronts are focused onto a square-law detector; in the Goddard instrument this detector is a HgCdTe photomixer cooled to liquid nitrogen temperatures. The detector output is proportional to the product of the E-vector amplitudes of the laser and source radiation. This product produces a time variable heterodyne voltage whose frequency is given by the absolute value of the difference between the source and LO frequencies. This so-called intermediate frequency (IF) falls in the radio frequency (RF) range, and thus the detector output is amplified and detected using conventional RF technology. The frequencies present in the optical spectrum near the LO frequency are down-converted into an RF spectrum. The Goddard instrument performs RF spectral analysis using 64 filters of 25 MHz FWHM, covering the IF spectrum from 25 to 1600 MHz. In addition, a tunable 64 channel bank of 5 MHz filters was available to measure any desired 320 MHz portion of the IF spectrum, but data from this higher resolution mode are not used here. All channels were registered simultaneously. Both of these filter banks provide a spectral resolution much less than the $\sim$185 MHz e-fold Doppler half-width of solar absorption features at these frequencies. This technique yields data of high spectral purity with excellent frequency stability. A number of problems which are often present in conventional solar spectrographs, such as "seeing" fluctuations in the spectrograph optics, have no effect in heterodyne spectroscopy. Further details of the Goddard heterodyne system, and of heterodyne spectroscopy in general, can be found in Kostiuk and Mumma (1983), and references therein.

b. Optical null-balancing

A significant aspect of these observations is that they were made in an optically null-balanced mode. In this mode the heterodyne optical system chops between the Sun and a temperature-calibrated blackbody source. We use an 8-12μm

filter in the optical path to reduce synchronously-detected shot noise in the heterodyne signal from both sources. The blackbody temperature is variable up to 1300K, and the solar signal is attenuated by sheets of ordinary polyethylene plastic (a continuous absorber), until its intensity roughly matches the intensity of the blackbody source. The blackbody temperature is then fine-adjusted until the heterodyne power from the two sources is equal to within 1%. The difference signal between the two sources is then measured and eventually expressed as (S-B)/B, where S is the attenuated solar heterodyne signal and B is the blackbody heterodyne signal. Because of the balancing process, the blackbody signal B is an excellent approximation to the attenuated solar continuum, and corrections for slight imbalance are easily made in the data reduction process. The quantity (S-B)/B therefore expresses the fractional line absorption for solar features. When observing very bright sources, this null-balanced mode restores the advantages obtained with Dicke-type radiometers (Dicke 1946). Using this technique, signal-to-noise ratios in excess of 10^4 have been obtained on the solar continuum at these frequencies (Mumma et al. 1983). Additional improvement can be obtained by using a hotter blackbody source, thereby reducing the need to attenuate the solar signal.

The spatial resolution obtained in heterodyne spectroscopy is the diffraction limit of the telescope, which in this case was 2 arc-seconds (1.22 λ/D). Our use of plastic sheets to attenuate the solar signal degrades this resolution somewhat, but this has no impact on our results, since we did not observe at the extreme limb.

c. Sideband folding

A complication which arises in the interpretation of heterodyne spectra is the problem of sideband folding. The heterodyne detector responds only to the absolute value of the frequency difference between the source and the LO. This means that the heterodyne power at each IF frequency is proportional to the sum of the source power at two frequencies located symmetrically about the LO frequency. This can be thought of as a "folding" of the monochromatic source spectrum about the LO frequency to form a double sideband spectrum. This sideband folding results in a distortion of the profiles of solar absorption features when the solar line is close to the LO frequency. However, by adopting

a line shape function it is possible to fit to the double sideband line profile, and extract the parameters of the monochromatic line with little ambiguity. In this paper we will, of necessity, illustrate the observed lines as double sideband spectra in our figures, but we will consistently refer only to monochromatic (single sideband) parameters when quoting the derived properties of the lines.

d. Choice of lines observed

The choice of lines which were observed in this investigation was dictated by the necessity of obtaining a favorable overlap between the solar OH features and the $^{14}C^{16}O_2$ laser frequencies. This restricts us to two v=0 and two v=1 lines. Two of these lines have been observed, the basic line parameters are given in Table I, and the observations are summarized in Table II. We will discuss each of these lines explicitly.

e. The v=1 R11(29.5)f line

Figure 1 shows a portion of the disk center photospheric spectrum near 885 cm^{-1}, taken with the Kitt Peak McMath FTS at 0.005 cm^{-1} resolution by D. Glenar, D. Jennings, and J. W. Brault. Several lines in the v=1, N =29 quartet of OH are seen in this spectrum. The R11(29.5)f line is seen to lie favorably near to the R(26) transition of $^{14}C^{16}O_2$, which is at 885.60530 cm^{-1} (Freed et al. 1980). Figure 2 illustrates heterodyne spectra in this region, made on two occasions separated by approximately one year. We have derived the parameters of the R11(29.5)f line by fitting the intensity data to a gaussian profile, with a linear baseline. We use a nonlinear least squares algorithim described by Bevington (1969). The fitting procedure extracts a line center frequency, line depth, line width, and baseline parameters. The frequencies we derive for this line from two disk center measurements (Figs. 2a and 2b) differ by only 0.00020 cm^{-1}, corresponding to a velocity difference of 66 meters/sec. At our spatial resolution, a velocity difference of this magnitude can easily be due to differences in the intrinsic solar velocity field. We obtain an average heliocentric solar frequency for this line of 885.6431 cm^{-1}. This frequency should be more accurate than the value from Goldman, Gillis and Coxon (1983), who calculate the frequency as 885.6456 cm^{-1}, based on molecular constants

derived from lower resolution solar data. Our fitting procedure also yields a line center residual intensity and width for this feature. We find that the line width exceeds the Doppler width and we attribute the excess broadening to the usual "microturbulence." The kinetic temperature in the line forming region ($\tau_{5000} \sim 0.07$) was taken to be 5050K (Saiedy 1960). This allows us to derive microturbulent values of $\sim$1.2 km/sec at disk center, and 1.9 km/sec at $\mu = \cos\theta = 0.3$, where the angle θ is taken between the line of sight and a line connecting the observed location with the solar center. Our data for this line, and for the v=0 line described below, are consistent with an increase in microturbulence with decreasing μ. However, we will not pursue this point, since this effect is well documented in the literature (Beckers 1981). It is of more interest to note that the line core residual intensity of this line does not depend significantly upon μ. Two observations at disk center, separated by a year of time (Figs. 2a and 2b), give residual intensities of 0.9770 and 0.9772. The residual intensity at $\mu = 0.3$ was derived to be 0.9772 (Fig. 2c), and so the depth of this line has not changed appreciably at $\mu = 0.3$. This behavior is in contrast to the behavior of the v=0 line described below. The good reproducibility of the data shown in Fig. 2 (compare Figs. 2a and 2b) lead us to believe that the technique used here has great potential as a tool for the precise monitoring of line shapes and Doppler shifts, even in relatively weak solar absorption features.

f. <u>The v=0 R22(24.5)e line</u>

Figure 3a shows the disk center solar spectrum at 0.005 cm^{-1} resolution near 839 cm^{-1}, as observed by D. Glenar, D. Jennings and J. W. Brault with the Kitt Peak McMath FTS. Figure 3b shows a region measured with our heterodyne spectrometer, at spectral resolution 0.00083 cm^{-1}. The v=0 R22(24.5)e line of OH occurs close to the P(32) transition of $^{14}C\,^{16}O_2$, which is at 839.1958 cm^{-1} (Freed et al. 1980). The OH line profiles shown on Fig. 3 were used to determine the heliocentric frequency of this line as 839.1922 cm^{-1}, and Sauval et al. (1984) list the line at 839.191 cm^{-1}. These measured values should supercede the value from Goldman, Gillis and Coxon (1983), who calculate its frequency as 839.1879 cm^{-1}. In subsequent fitting to other observations of this line we constrain the heliocentric line frequency to the value we derive above, making adjustments for solar rotation using the model of Howard and Harvey

(1970). The reason for this procedure is that in much of our data this line occurs quite close to the LO, in which case its frequency is poorly determined by a least squares fit to the double sideband line profile. We determine other parameters for this line by least squares fitting of a double sideband Voigt profile. This line is sufficiently strong that a small amount of pressure broadening can be discerned in the line wings, and fitting of a gaussian profile is inadequate. We should note that the sideband folding present for this line forces us to derive the line parameters by fitting to the intensity profile, not to the logarithm of the intensity profile. However, since the line is weak ($\sim$8%), this procedure is an excellent approximation. The only significant error introduced is that we obtain microturbulent values which are $\sim$0.1 km/sec too large. Table II includes the results of the least squares fitting to the intensity profiles of both lines.

A more complete series of center-to-limb observations was obtained for this v=0 line and a profile at μ=0.3 is illustrated in Fig. 3c. Unlike the v=1 line, this lower excitation line becomes significantly stronger at the limb. The line core residual intensity is shown as a function of μ in Fig. 4. It can be seen that at $\mu \leq 0.4$ the line core residual intensity drops sharply from 0.92, reaching 0.89 at μ=0.2. At disk center the core of this line is formed in the upper photosphere at $\tau_{5000} \sim 10^{-2}$. In this region the temperature gradient should be decreasing, which should lead to weaker lines at smaller values of μ. Calculations using model atmospheres confirm this expectation. Fig. 4 shows the line core residual intensities expected for both the v=0 and v=1 line, based on the Holweger-Muller model atmosphere. This model fails to reproduce the center-to-limb behavior of the v=0 line, although it successfully reproduces the disk-center excitation conditions of the v=0 data given by Goldman et al. (1983), and the v=0, 1, 2 and 3 data given by Sauval et al. (1984). Model atmospheres having steeper temperature gradients, such as the Vernazza et al. (1976) model, are able to reduce, but not eliminate, the discrepancy with our v=0 center-to-limb data. These models, however, are too cool to account for the excitation of these lines at disk center.

The equivalent width of this line can be derived from the parameters of the fitted Voigt profile given in Table II. This gives an average value of 1.55 mK (milli-Kaysers, 1 mK = 10^{-3} cm^{-1}) at disk center, which requires a solar oxygen

abundance of 9.06. Both our equivalent width and oxygen abundance are larger than the values quoted by Goldman et al. (1982) and Sauval et al. (1984) for this line. Our disk center data show that line absorption can be detected as far as 30 mK (≈900 MHz) from line center; this effect does not appear in the FTS profile of a similar line illustrated by Sauval et al. (1984). However, the FTS data of Fig. 3a do show a slope in this region due to the presence of a telluric water line at 839.871 cm^{-1}. We have considered whether the wing of this water line can be affecting our observations, and we conclude that it does not. It must be remembered that a linear slope in the monochromatic (single sideband) spectrum appears as a flat baseline in a double sideband spectrum; only quadratic terms in the monochromatic spectrum produce slopes in the double sideband baseline. In the present case we calculate that the telluric water line should produce a change of 0.04% over the 1600 MHz spanned by our data. Moreover, the sense of this effect is to produce a larger intensity at the LO than at 1600 MHz. This is just the opposite of the effect seen in our solar data, so we conclude that the 839.871 cm^{-1} water line has not affected our observations. Our data therefore suggest that the equivalent widths from the FTS data of both Goldman et al. (1983) and Sauval et al. (1984) may be systematically low for the v=0 lines. However, since we were able to observe only a single v=0 line, we cannot be too adamant on this point. This matter bears further investigation.

g. Errors

In fitting Voigt profiles to the observed lines, the uncertainty in the derived line parameters cannot be given by an analytic expression. We have therefore estimated random errors using the following procedure. First we calculate the level of random error in the data, by subtracting the best fit from the observed points. We then repeatedly and independently perturb the original data by adding additional gaussian random noise of this magnitude, and re-fit the line parameters. In this way we can calculate the dispersion in the fitted parameters which results from additional random perturbations of the original data. Since the data quality is relatively uniform, these errors are relatively constant from line to line. We obtain typical random errors of $\pm 0.05\%$ in line core residual intensity, ± 5 MHz in $\Delta\nu_D$ and ± 0.03 in the ratio of damping to Doppler width, a. Systematic errors will also occur due to imperfect

repeatability of the blackbody intensity, detector response, and similar effects. The effect of most of these errors is greatly reduced by the balancing process. The most important source of systematic error in these data is the repeatability of the reference blackbody intensity. We estimate that this leads to errors in line core residual intensity of order 0.1%, and measurements of the v=1 line (Fig. 2) support this estimate. The v=0 line core, however, shows variations as large as 0.5% in residual intensity, at a given value of μ, from measurement to measurement. We suspect these variations are real changes in the line depth. We note that integration times for our data were in the range of 5-10 minutes, and so we might expect to see line depth variations due to the 5-minute oscillations.

III. ANALYSIS

a. Limb darkening functions

Any analysis of the center-to-limb behavior of these OH rotational lines should consider the center-to-limb behavior of the continuum intensity in the 10μm region. The 10μm continuum limb darkening has been measured by Pierce et al. (1950), Saiedy (1960), and by Lena (1970). The data by Pierce et al. and by Saiedy were not made on the McMath solar telescope, and they do not extend to the extreme limb ($\cos\theta < 0.2$). However, the observations by Lena were made on the McMath telescope using a high resolution scanning technique, and these data extend to within a few arc-seconds of the limb. Since atmospheric seeing is better at 10μm than in the visible (e.g. Turon and Lena 1970), these data should be reliable and may be valuable in constraining models of the upper photosphere.

Fig. 5 shows the 10μm limb darkening data from Pierce et al. (1950), Saiedy (1960), and Lena (1970). In the region $0.3 > \mu > 0.2$ the Pierce et al. and Lena data are in disagreement; the implications of this discrepancy are noted below. Although Lena's data extend to the extreme limb, his measurements at $\mu < 0.14$ show a sharp drop in intensity due to the effect of finite spatial resolution. Lena discusses the removal of this effect by deconvolution, to arrive at the true limb darkening function. While we have no criticisms of Lena's procedure, we have conservatively used his data only for $\mu > 0.14$ so that our conclusions are not dependent on the details of this deconvolution.

An effective way to circumvent the observational problems encountered at the extreme limb is to observe the monochromatic limb darkening function in the core of an OH absorption line. In this case the additional opacity present in the line allows us to probe the upper photosphere without observing particularly close to the limb. Fig. 5 shows the limb darkening function which we obtain for the core of the v=0 R22(24.5)e line at 839.192 cm^{-1}. Since we measure only the relative depth of this line at any μ, we have adopted a value for the continuum intensity at each μ in order to reconstruct the line core limb darkening function. Since the available continuum measurements show systematic differences between investigators, we must shoulder the burden of deciding between the available measurements. We adopt the data of Pierce et al. (1950) for $\mu > 0.3$ and Lena's (1970) data for $\mu < 0.3$. With this choice we can convert our measures of relative line depth (Fig. 4) into a limb darkening function for the line core. In implementing this procedure we ignored the (negligibly small) change in the continuum limb darkening function between 10.2 and 11.92μm. For example, at $\mu=0.2$ the line core residual intensity we measure as 0.899 (see Fig. 4), whereas the continuum intensity at this point, from Fig. 5, is 0.92 of the disk center intensity. This implies that the line core intensity at $\mu=0.2$ is 0.827 relative to the disk center continuum intensity. Adopting T=5050K for the continuum disk center brightness temperature gives a line core brightness temperature of T=4270K at $\mu=0.2$. Since we expect both the OH lines and the continuum to be in LTE, this evidence would seem to eliminate those one-dimensional models of the upper photosphere which have temperature minima above 4270K.

b. Radiative transfer inversion calculations

Having adopted the continuum and line core limb darkening functions from Fig. 5, we wish to mathematically invert these relations so as to investigate the temperature structure of the upper photosphere. In so doing, we must recognize that such inversions can, in principle, give only the coarse structure of the atmosphere (Bohm 1961). With the present data we can derive no information about the atmospheric structure on scales less than ~ 1.2 in $\ln \tau_\nu$. In the line core, however, this optical depth limit translates into much finer structure in a temperature/pressure relation. The line opacity greatly reduces the photon mean-free-path, which in principle allows the extraction of high

resolution information from line core limb darkening measurements. However, such measurements are seldom used for this purpose because of the stringent requirements on spectral purity. In the present case, however, we believe that our data meet these requirements.

Inversion of these data to obtain $T(\tau)$ relations for the line core and continuum proceeds as follows. We write the emergent intensity as:

$$I(\mu) = \sum_{i=1}^{N} S_i (e^{-\tau_{i-1}/\mu} - e^{-\tau_i/\mu}) \qquad (1)$$

where the S_i represent the source functions we wish to determine, τ_i represent optical depth points, and N is determined from Bohm's (1961) criterion (his Eq. 15). In what follows we will take N=4 and τ_i = 0, 1/3, 1, 3, and 9 for i=0 to 4. With this choice of the τ_i, (1) reduces to a set of linear equations. Since we have many measurements of $I(\mu)$, these equations are formally (but not physically) overdetermined. We solve for an optimum set of S_i using a minimax criterion (Barrodale and Phillips 1975). We tested this quadrature procedure by inverting values of $I(\mu)$ for predetermined sets of S_i, and verified that this procedure is capable of retrieving the predetermined S_i values.

When inverting the observed limb darkening curves, we used an average intensity at each μ, obtained as an eye estimate of the Fig. 5 data. Average intensities for (typically) 8-10 values of μ were estimated and input to the inversion procedure. The resultant model was always found to reproduce the input intensities to a much higher precision than the errors in the observations would justify. In order to make realistic error estimates for the retrieved source functions, we repeatedly and independently perturbed the input values for average intensity at each μ. We did this by adding gaussian random noise to these values, with noise amplitude equal to the scatter in the observed data (typically 0.5%). The resultant dispersion in the retrieved source functions gave an error estimate for the model source functions at each depth. The results of inverting the continuum and line core limb darkening data are given in Table III. Since we expect LTE, we have expressed the S_i as local kinetic temperatures.

IV. DISCUSSION

a. Implications for the solar emission lines

The 10-12μm region of the solar spectrum has recently been found to contain emission features (Murcray et al. 1981, Brault and Noyes 1983) which Chang and Noyes (1983) identified as transitions between high-lying Rydberg states of neutral magnesium and aluminum. We believe that the heterodyne (Fig. 2) and FTS (Fig. 1) observations of the v=1 R11(29.5)f line may provide significant insight into the formation mechanism of these emission features. To see this, requires some discussion.

The oxygen abundance derived from the heterodyne observations (Table II) of the R11(29.5)f line, using the Holweger-Muller model atmosphere, is 8.63, much less than the value of 8.91 which Sauval et al. (1984) find to be consistent with the vast majority of OH rotational lines. Sauval et al. do not list an equivalent width for the R11(29.5)f line, noting instead that telluric HNO_3 absorption occurs in this region. However, our heterodyne spectra show that this solar line has a symmetric, gaussian, profile, and we do not believe that our data are significantly affected by telluric absorption. In order to be consistent with an oxygen abundance of 8.91, the depth of this line would have to be $\gtrsim$ 4%, instead of the 2.28% which we obtain. This difference is greatly in excess of any plausible error in our observations.

This phenomenon of occasional low abundance values from these OH rotational lines was first noted by Sauval et al., who observed that this occurs for those OH lines which are in close proximity to the solar emission features listed by Brault and Noyes (1983). Sauval et al. remark that the emission features are accompanied by absorption wings, and they postulate that these absorption wings lower the local continuum, without affecting the emergent intensity in the OH line core. This will weaken the OH features, as required, as long as the opacity introduced by the absorption wing has a larger effect in the continuum-forming region of the atmosphere than it does in the OH line-forming region. In the present instance, we also find that the v=1 R11(29.5)f line lies in close proximity to a solar emission line. Brault and Noyes (1983) list an emission feature at 885.524 cm^{-1}, which Chang and Noyes (1983) identify with the

9j-7i transition of MgI. This emission feature is weak, amounting to 3% of the continuum at μ=0.14 (Brault and Noyes 1983). Indeed, it is not visible in the disk-center FTS spectrum illustrated in Fig. 1. Nevertheless, it has apparently perturbed the R11(29.5)f line of OH to a significant degree. Moreover, the mechanism proposed by Sauval et al. will not explain this anomaly. The Fig. 1 FTS spectrum clearly shows that the R11(29.5)f line of OH is weak, not because the continuum is lower, but because the specific intensity in the line core is greater than the values for the other lines in this quartet. The intensity emergent at any frequency is determined by an integral of the source function over optical depth. Therefore it must happen that either the optical depths or source function for the OH line core have been perturbed by the presence of the emission line. This can only happen if the 9j and 7i level populations in MgI are not in a thermal ratio in those regions of the photosphere where the OH line core is formed ($\tau_{5000} \sim 0.07$). This inference may be useful in constructing models of the emission line formation process.

b. Thermal fluctuations in the upper photosphere

In interpreting the model atmospheres given in Table III, we must keep in mind that the continuum data which we have used were the result of a choice between the results of three investigations, which differed systematically. The data by Pierce et al., for example, give an intensity some 2% greater than Lena's measurements near μ = 0.2. If we had adopted the Pierce et al. data in this region, our line core inversions would also have been affected, because the line core limb darkening relation is derived from the continuum limb darkening function, in combination with our relative line depth measurements. With a different choice for the continuum limb darkening function, our inversion results are quantitatively, but not qualitatively, different and our conclusions are unchanged. The fact that our measurements of relative line depth (Fig. 4) show the v=0 line to strengthen at the limb is the essential fact which drives our conclusions.

Fig. 6 shows the results of Table III plotted on a common optical depth scale. In constructing this common optical depth scale, we calculated line center and continuum opacities in the Holweger-Muller model photosphere, with an oxygen abundance of 9.06. This allowed us to determine the ratio of line core

to continuum optical depth as a function of continuum optical depth, and we assumed that this relation also held for our retrieved model. The shaded regions on Fig. 6 denote the extent of $\pm 1_\sigma$ temperature uncertainties in our retrieved model. For continuum optical depths exceeding 1/3, the errors are large and our retrievals are not inconsistent with the Holweger-Muller model. However, at continuum optical depths less than 1/3, our inversions imply deviations from the Holweger-Muller model as large as ±800K. It is well known that radiative transfer inversions can yield spurious temperature oscillations if too fine a division in optical depth is attempted. However, we have tested our inversion procedure using "synthetic" data, and we claim that the variations we retrieve are indeed needed to fit our data.

There are two ways to interpret the thermal fluctuations which we infer from our center-to-limb data. First, we might view the upper photosphere as horizontally homogenous, as is assumed in a one-dimensional model. Although the requisite thermal fluctuations are quite large, we are not able to eliminate this possibility based on data which are available to us. Moreover, the vertical temperature gradients, $|d\ln T/d\ln P|$, attain maximum values of ~ 0.32, which is large but not superadiabatic. However, there is no explanation at hand as to how such large deviations from radiative equilibrium can be produced. Travelling acoustic waves of periods $\sim$20-60 sec can produce $\sim \pm$ 200K deviations from radiative equilibrium (Ulmschneider and Kalkofen 1977), and these might be observable in high time resolution data. However, our total data set required hours of real-time observing, over a large fraction of a solar radius, and we consequently require a mechanism for producing large average deviations from radiative equilibrium. In this respect, acoustic waves are not a viable candidate (e.g. see Jordan 1981). A second way to interpret our results is in the context of horizontal inhomogeneities on a spatial scale which is unresolved by our data. In this case the ± 800K variations which we infer may not be a numerically accurate estimate, since the atmospheric geometry differs from the assumptions of our inversion algorithm. This interpretation is easier to accomodate since the horizontal temperature fluctuations can be sustained by the presence of magnetic flux tubes, and the thermal bifurcation model of Ayres (1981). Also, recent submillimeter observations of the solar limb (Lindsey et al. 1983, 1984) have indicated the need for a horizontally inhomogenous chromosphere just above the temperature minimum. Our results may indicate that

these inhomogeneities extend as deep as $\tau_{5000} \sim 10^{-3} - 10^{-2}$. Solar spectroscopy in the low-J far-infrared lines of OH (Brown et al. 1982) could contribute significantly to further understanding of the temperature minimum region.

Acknowledgements

We thank Drs. D. Glenar, D. Jennings, and J. W. Brault for allowing us to reproduce and discuss portions of their unpublished FTS spectra. Dr. Aaron Goldman kindly supplied us with a list of OH line frequencies and excitation potentials. We are grateful to Dr. W. Livingston for relinquishing some telescope time to us. We benefitted from discussions with Dr. Barney Conrath on the subject of radiative transfer inversions. We thank the support staff of Kitt Peak National Observatory for their patient support of a complex and demanding experiment.

REFERENCES

Ayres, T. R. 1981, Astrophys. Jour. 244, 1064.

Ayres, T. R. and Linsky, J. L. 1976, Astrophys. Jour. 205, 874.

Ayres, T. R. and Testerman, L. 1981, Astrophys. Jour., 245, 1124.

Barrodale, I. and Phillips, C. 1975, ACM Transactions on Mathematical Software, 1, 264.

Beckers, J. M. 1981, in The Sun as a Star, S. Jordan ed. NASA SP-450, p. 11.

Bevington, P. R. 1969, Data Reduction and Error Analysis for the Physical Sciences, McGraw-Hill Inc., New York, NY.

Bohm, K. 1961, Astrophys. Jour., 134, 264.

Brault, J. W. and Noyes, R. W. 1983, Astrophys. Jour. (Lett.), 269, L61.

Brown, J. M., Schubert, J. E., Evenson, K. M. and Radford, H. E., 1982, Astrophys. Jour. 258, 899.

Carbon, D. F., Milkey, R. W. and Heasley, J. N. 1976, Astrophys. Jour. 207, 253.

Carlone, C. and Dalby, F. W. 1969, Can. Jour. Phys. 47, 1945.

Chang, E. S. and Noyes, R. W. 1983, Astrophys. Jour. (Lett.) 275, L11.

De Jager, C. 1975, Space Science Reviews 17, 645.

Dicke, R. H. 1946, Rev. Sci. Instr. 17, 268.

Freed, C., Bradley, L. C. and O'Donnell, R. G. 1970, IEEE J. Quantum Electron. QE-16, 1195.

Gay, J. and Journet, A. 1973, Nature Phys. Sci. 241, 32.

Goldman, A. and Gillis, J. R. 1981, Jour. Quan. Spec. Rad. Trans. 25, 111.

Goldman, A., Murcray, D. G., Lambert, D. L. and Dominy, J. F. 1983, Mon. Not. Roy. Astr. Soc. 203, 767.

Goldman, A., Murcray, F. J., Gillis, J. R. and Murcray, D. G. 1981, Astrophys. Jour. (Lett.) 248, L133.

Goldman, A., Gillis, J. R. and Coxon, J. A. 1983, Jour. Quan. Spec. Rad. Trans., 29, 469.

Hinckle, K. H. and Lambert, D. L. 1975, Mon. Not. Roy. Astr. Soc. 170, 447.

Holweger, H. and Müller, E. A. 1974, Solar Phys. 39, 19.

Howard, R. and Harvey, J., 1970, Solar Phys. 12, 23.

Jordan, S. 1981, in The Sun as a Star, S. Jordan, ed. NASA SP-450, 301.

Kostiuk, T. and Mumma, M. J. 1983, Applied Optics 22, 2644.

Lindsey, C., Becklin, E. E., Jeffries, J. T., Orral, F. Q., Werner, M. W. and Gatley, I. 1983, Astrophys. Jour. (Lett.) 264, L25.

Lindsey, C., DeGraauw, T., DeVries, C. and Lindholm, S. 1984, Astrophys. Jour. 277, 424.

McElroy, J. H. 1972, Applied Optics 11, 1619.

Meerts, W. L. and Dymanus, A., 1973 Chem. Phys. (Lett.) 23, 45.

Mies, F. H. 1974, Jour. Molec. Spectros. 53, 150.

Mumma, M. J., Rogers, J. D., Kostiuk, T., Deming, D., Hillman, J. J., and Zipoy, D., 1983, Science 221, 268.

Murcray, F. J., Goldman, A., Murcray, F. H., Bradford, C. M., Murcray, D. G., Cofffey, M. T., and Mankin, W. G. 1981, Astrophys. Jour. (Lett.) 247, L97.

Pierce, A. K., McMath, R. R., Goldberg, L. and Mohler, O. C. 1950, Astrophys. Jour. 112, 289.

Saiedy, F. 1960, Mon. Not. Roy. Astr. Soc. 121, 483.

Sauval, A. J., Grevesse, N., Brault, J. W., Stokes, G. M. and Zander, R. 1984,

Astrophys. Jour. (Lett.), in press.

Spruit, H. C. 1981, in The Sun as a Star, S. Jordan, ed. NASA SP-450, 385.

Stevens, W. J., Das, G., Wahl, A. C., Krauss, M. and Neumann, D. 1974, Jour. Chem. Phys. 61, 3686.

Turon, P. J. and Lena, P. J. 1970, Solar Phys. 14, 112.

Ulmschneider, P. and Kalkofen, W. 1977, Astron. Astrophys. 57, 199.

Vernazza, J. E., Avrett, E. H., Loeser, R. 1976, Astrophys. Jour. 30, 1.

Veth, C., deGraauw, Th., Shelton, J. C. and van de Stadt, H. 1973, Astr. Astrophys. 26, 479.

Werner, H. J., Rosmus, P. and Reinsch, E. A. 1983, J. Chem. Phys. 79, 905.

TABLE I. Parameters for the lines observed; E'' is the lower state excitation in cm^{-1} from Goldman, Gillis and Coxon (1983). A dipole moment of 1.6676 Debye was adopted for v=0 (Meerts and Dynamus 1969), and 1.6743 Debye was used for v=1 (Mies 1974). The line frequencies are heliocentric frequencies obtained from our observations.

LINE	FREQUENCY (cm^{-1})	E"(cm^{-1})	log gf
v=0 R22(24.5)e	839.1922	11,315	-1.554
v=1 R11(29.5)f	885.6431	17,766	-1.439

TABLE II. Summary of line profile observations. Line parameters were derived by fitting the observations to a Voigt profile, H(a,v). $\Delta\nu_D$ is the e-fold Doppler half-width. The observations are listed in chronological order.

			LINE		MICROTURBULENCE	
DATE	LINE	μ	DEPTH(%)	$\Delta\nu_D$(MHz)	(KM/SEC)	a
5 May 1982	v=1 R11(29.5)f	1.00	2.30	225	1.3	0
6 May 1982	v=0 R22(24.5)e	1.00	7.72	260	2.2	0.05
		0.714	7.17	257	2.1	0.25
		0.436	7.95	283	2.5	0.18
2 April 1983	v=0 R22(24.5)e	1.00	8.46	208	1.1	0.41
		0.695	7.39	264	2.2	0.22
		0.203	10.58	297	2.8	0.17
		0.302	9.41	265	2.3	0.32
		0.248	9.14	288	2.6	0.28
		0.398	7.81	265	2.2	0.35
		0.497	7.23	315	3.0	0.19
		0.598	8.05	244	1.9	0.44
		0.797	8.50	223	1.5	0.48
		1.00	8.73	190	0.5	0.67
		0.248	9.59	231	1.6	0.64
		0.302	8.65	276	2.4	0.24
		0.302	10.31	231	1.6	0.53
	v=1 R11(29.5)f	1.00	2.28	218	1.1	0
		0.302	2.28	261	1.9	0

TABLE III. Results of radiative transfer inversions.

Optical Depth	Temperature (Kelvins) Line core data	Continuum data
0 - 1/3	3950 ± 103	4479 ± 56
1/3 - 1	5609 ± 278	5639 ± 228
1 - 3	4061 ± 455	4560 ± 497
3 - 9	6070 ± 1293	7365 ± 2713

Figure 1. FTS spectrum of the region near the v=1, N''=29 quartet of solar OH. The position of the R(26) line of $^{14}C^{16}O_2$, used as a local oscillator for the heterodyne observations, is noted. The position of a weak solar emission line due to MgI is also noted, although the emission line is not detectable in this spectrum.

Figure 2. Heterodyne observations of the v=1 R11(29.5)f line of OH from the photosphere. The ordinate is relative intensity in the double sideband spectrum, whereas the quoted line parameters apply to the single sideband (monochromatic) spectrum. The fitted profiles are Gaussian, with linear baselines. The 1983 observations contain correlated noise near the local oscillator frequency.

Figure 3. A photospheric disk center spectrum at 0.005 cm^{-1} resolution is shown in A), and heterodyne observations of the region near the v=0 R22(24.5)e line of OH are illustrated in B and C. The ordinate for the heterodyne spectra is relative intensity in the double sideband spectrum. The heterodyne spectra are fitted with Voigt profiles, with a flat baseline. The quoted line parameters refer to the single sideband (monochromatic) spectrum. The NO_2 line is stratospheric, and occurs at 839.173 cm^{-1}.

Figure 4. Center to limb behavior of the v=1 R11(29.5)f line and v=0 R22(24.5)e line. The ordinate is the line core intensity divided by the continuum intensity. The dashed line shows the behavior expected from the Holweger-Muller photospheric model, and the solid line was computed from the models given in Table III.

Figure 5. Center-to-limb behavior of the photospheric continuum intensity near 11μm, and of the intensity in the core of the v=0 R22(24.5)e line of OH. The ordinate is intensity divided by the μ=1 continuum intensity, and the right hand scale gives the 839 cm^{-1} brightness temperature. The dashed line shows the relations predicted by the Holweger-Muller model, and the solid line was computed from the models given in Table III.

Figure 6. Model of the upper photosphere obtained by placing the line core and continuum inversion models (Table III) on a common optical depth scale. The shaded regions denote the extent of $\pm 1\sigma$ temperature uncertainties. The dashed line emphasizes the temperature fluctuations observed at small optical depth.

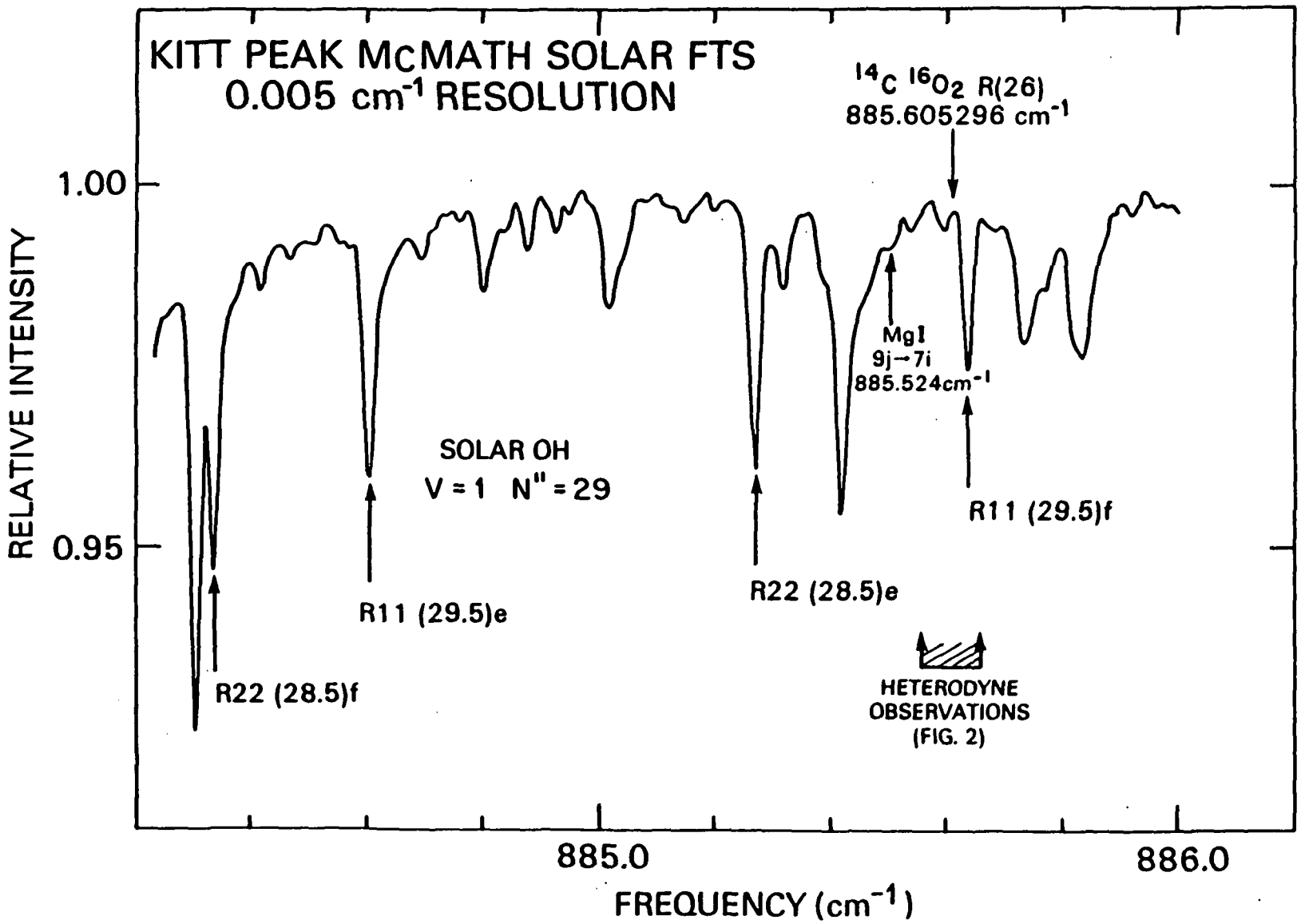
KITT PEAK McMATH SOLAR FTS
0.005 cm-1 RESOLUTION
14C 16O2 R(26)
885.605296 cm-1
1.00
0.95
RELATIVE INTENSITY
MgI
9j–7i
885.524cm-1
SOLAR OH
V = 1 N" = 29
R11 (29.5)f
R11 (29.5)e
R22 (28.5)e
R22 (28.5)f
HETERODYNE
OBSERVATIONS
(FIG. 2)
885.0
886.0
FREQUENCY (cm-1)

Fig. 1

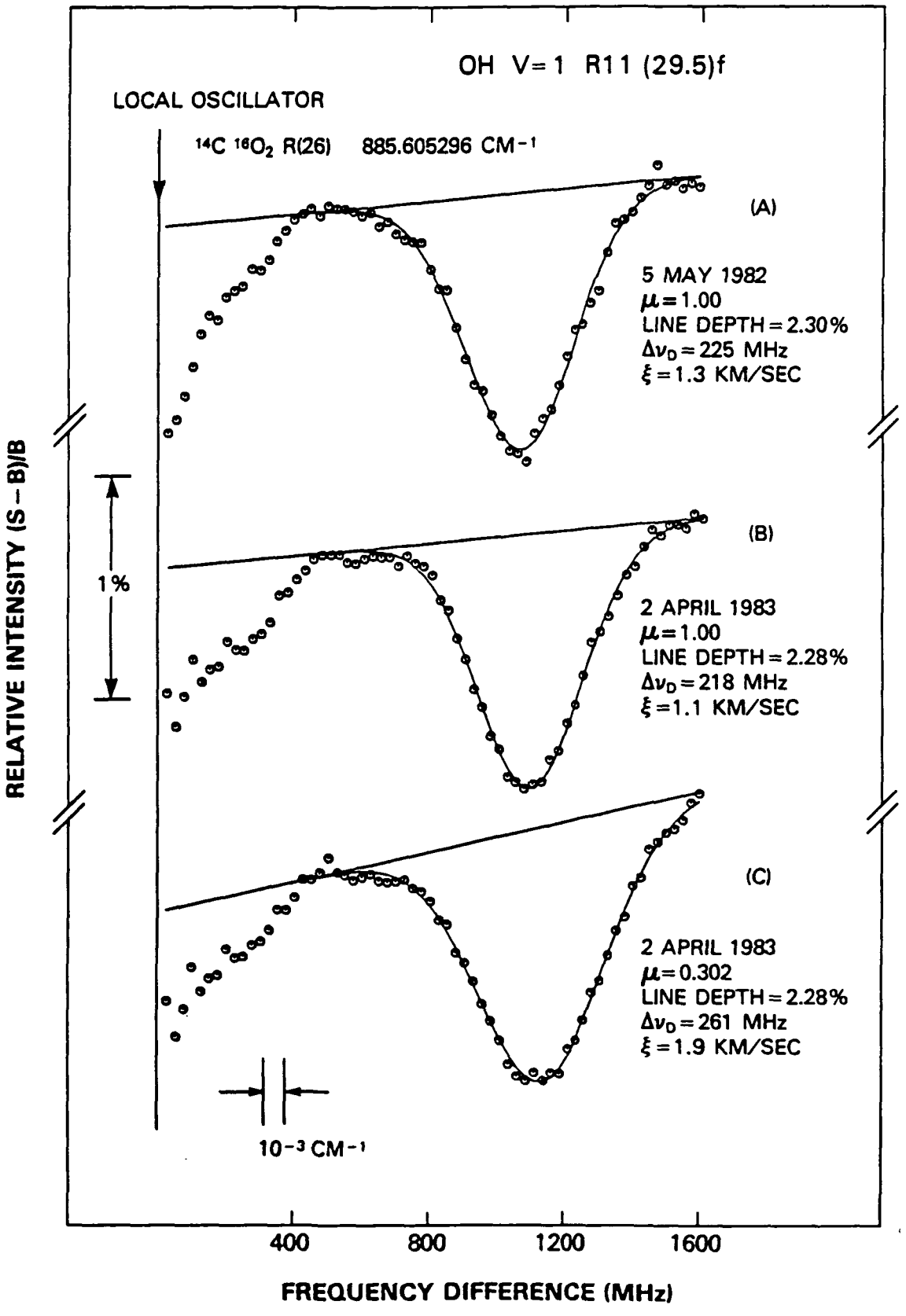
OH V=1 R11 (29.5)f
LOCAL OSCILLATOR
$^{14}C\ ^{16}O_2$ R(26) 885.605296 CM^{-1}
(A)
5 MAY 1982
μ=1.00
LINE DEPTH=2.30%
$\Delta\nu_D$=225 MHz
ξ=1.3 KM/SEC
(B)
2 APRIL 1983
μ=1.00
LINE DEPTH=2.28%
$\Delta\nu_D$=218 MHz
ξ=1.1 KM/SEC
(C)
2 APRIL 1983
μ=0.302
LINE DEPTH=2.28%
$\Delta\nu_D$=261 MHz
ξ=1.9 KM/SEC
1%
10^{-3} CM^{-1}
RELATIVE INTENSITY (S−B)/B
400
800
1200
1600
FREQUENCY DIFFERENCE (MHz)

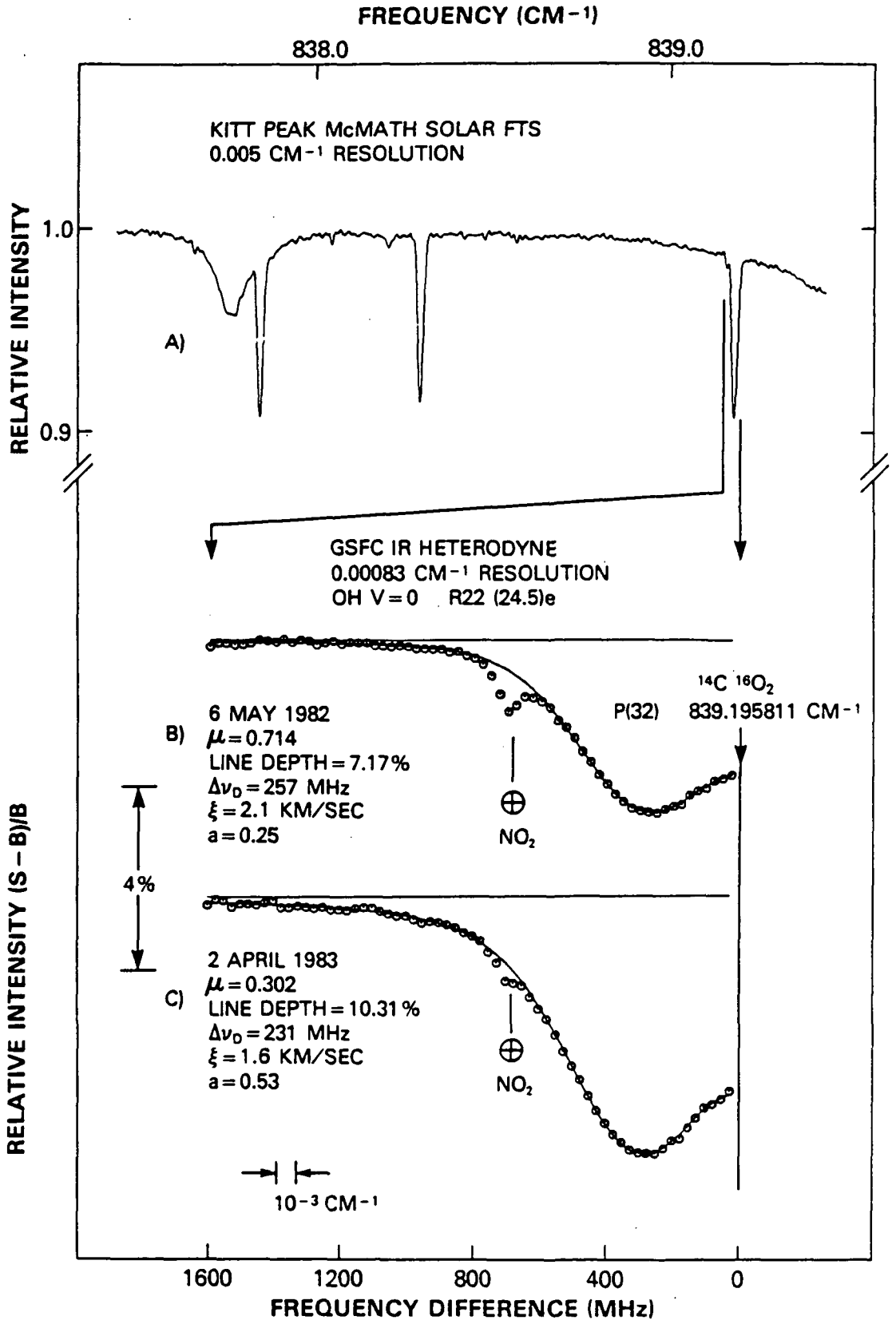
FREQUENCY (CM⁻¹)
838.0
839.0
KITT PEAK McMATH SOLAR FTS
0.005 CM⁻¹ RESOLUTION
RELATIVE INTENSITY
1.0
0.9
A)
GSFC IR HETERODYNE
0.00083 CM⁻¹ RESOLUTION
OH V=0 R22 (24.5)e
$^{14}C\,^{16}O_2$
P(32) 839.195811 CM⁻¹
6 MAY 1982
B) μ=0.714
LINE DEPTH=7.17%
Δν_D=257 MHz
ξ=2.1 KM/SEC
a=0.25
NO₂
4%
2 APRIL 1983
C) μ=0.302
LINE DEPTH=10.31%
Δν_D=231 MHz
ξ=1.6 KM/SEC
a=0.53
NO₂
10⁻³ CM⁻¹
RELATIVE INTENSITY (S-B)/B
1600
1200
800
400
0
FREQUENCY DIFFERENCE (MHz)

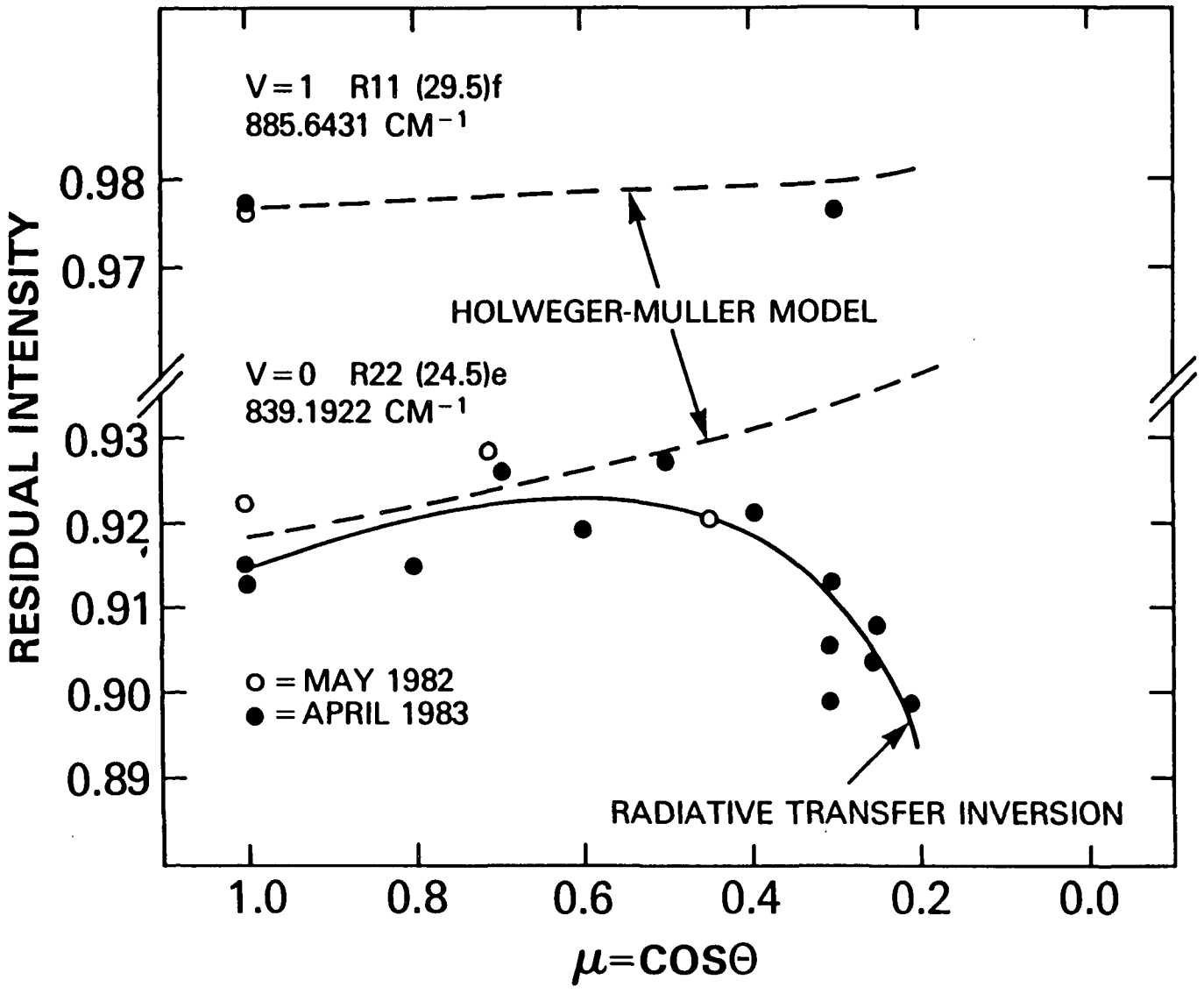
V=1 R11 (29.5)f
885.6431 CM⁻¹
V=0 R22 (24.5)e
839.1922 CM⁻¹
HOLWEGER-MULLER MODEL
RADIATIVE TRANSFER INVERSION
o = MAY 1982
● = APRIL 1983
RESIDUAL INTENSITY
0.98
0.97
0.93
0.92
0.91
0.90
0.89
1.0
0.8
0.6
0.4
0.2
0.0
μ=COSΘ

Fig. 4

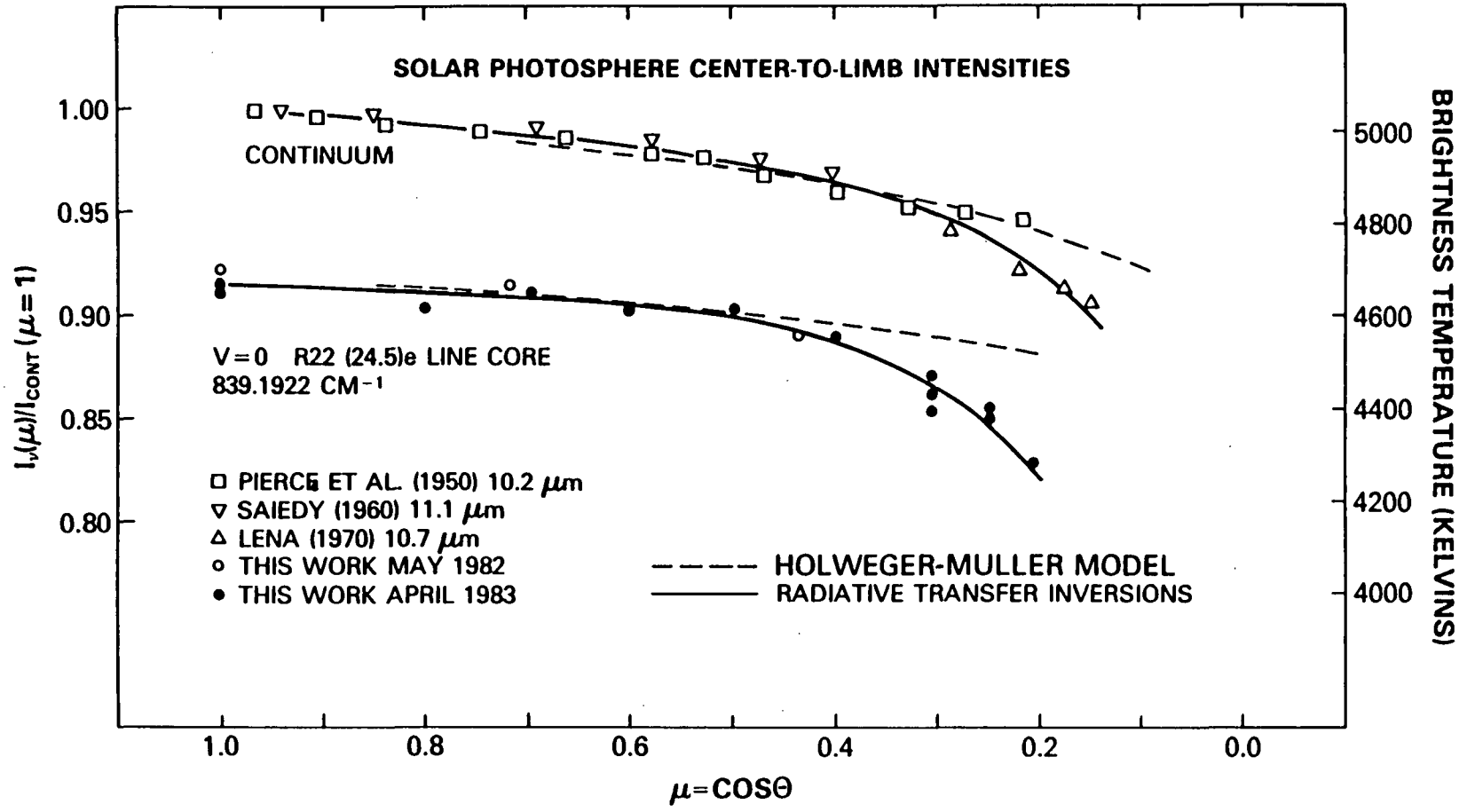
SOLAR PHOTOSPHERE CENTER-TO-LIMB INTENSITIES
CONTINUUM
V=0 R22 (24.5)e LINE CORE
839.1922 CM⁻¹
PIERCE ET AL. (1950) 10.2 μm
SAIEDY (1960) 11.1 μm
LENA (1970) 10.7 μm
THIS WORK MAY 1982
THIS WORK APRIL 1983
HOLWEGER-MULLER MODEL
RADIATIVE TRANSFER INVERSIONS
1.00
0.95
0.90
0.85
0.80
5000
4800
4600
4400
4200
4000
1.0
0.8
0.6
0.4
0.2
0.0
μ=COSΘ
BRIGHTNESS TEMPERATURE (KELVINS)

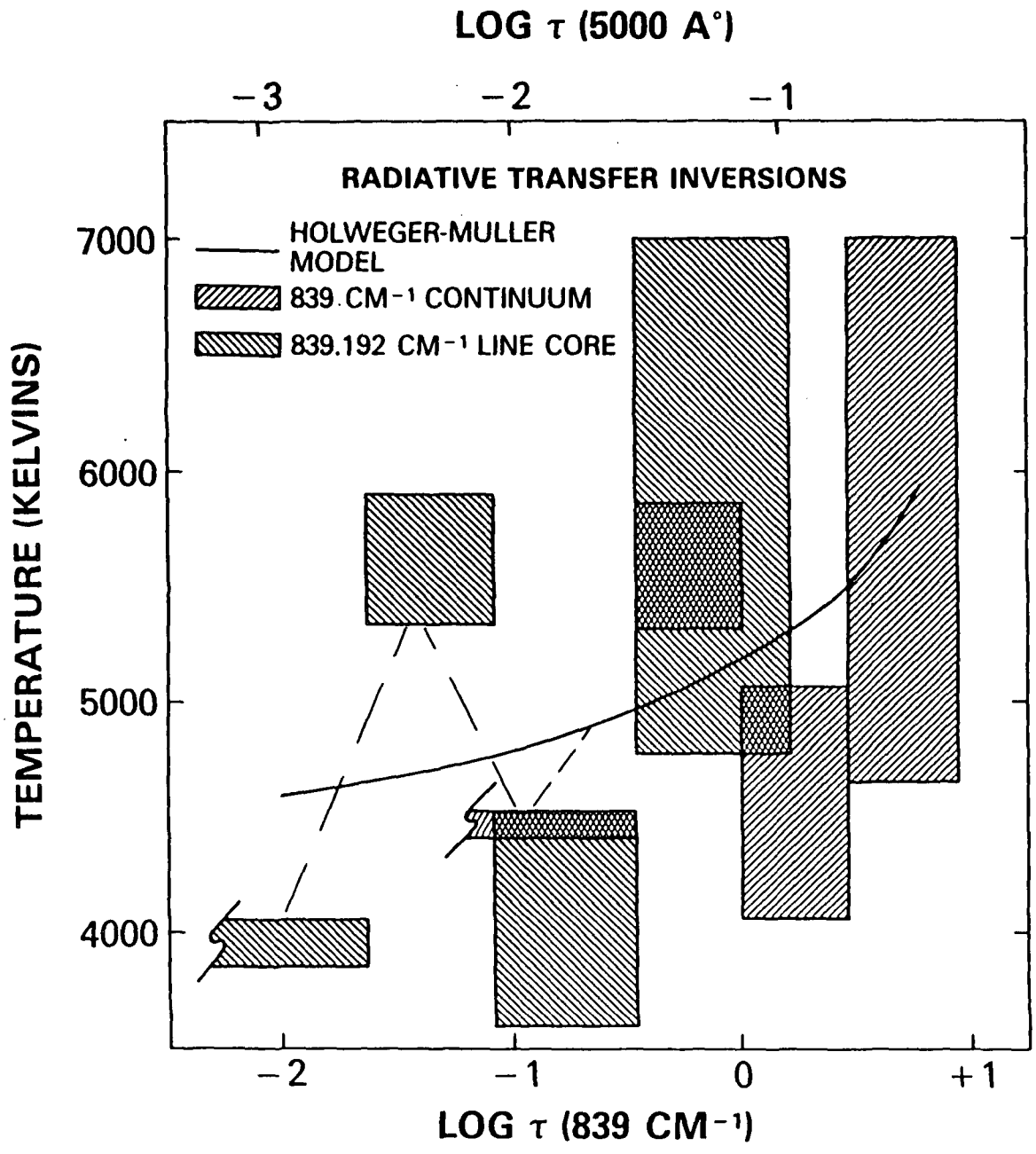
LOG τ (5000 A°)
−3
−2
−1
RADIATIVE TRANSFER INVERSIONS
HOLWEGER-MULLER MODEL
839 CM⁻¹ CONTINUUM
839.192 CM⁻¹ LINE CORE
7000
6000
5000
4000
TEMPERATURE (KELVINS)
−2
−1
0
+1
LOG τ (839 CM⁻¹)

Fig. 6

BIBLIOGRAPHIC DATA SHEET

1. Report No.	2. Government Accession No.	3. Recipient's Catalog No.
TM #68128		

4. Title and Subtitle	5. Report Date
Thermal Bifurcation in the Upper Solar Photosphere Inferred from Heterodyne Spectroscopy of OH Rotational Lines	June 1984
	6. Performing Organization Code 693
7. Author(s) D. Deming, John J. Hillman, Theodor Kostiuk, and Michael J. Mumma	8. Performing Organization Report No.
9. Performing Organization Name and Address Laboratory for Extraterrestrial Physics Infrared and Radio Astronomy Branch	10. Work Unit No.
	11. Contract or Grant No.
	13. Type of Report and Period Covered
12. Sponsoring Agency Name and Address	
	14. Sponsoring Agency Code

15. Supplementary Notes

16. Abstract

See attached.

17. Key Words (Selected by Author(s))	18. Distribution Statement

19. Security Classif. (of this report)	20. Security Classif. (of this page)	21. No. of Pages	22. Price*
		30	

*For sale by the National Technical Information Service, Springfield, Virginia 22161